Sensitivity of the EDML ice core chronology to the geothermal heat flux

O. Rybak[1,3], P. Huybrechts[1,2]

[1]Alfred-Wegener-Institut für Polar- und Meeresforschung, Bremerhaven, Germany

[2]Vrije Universiteit Brussel, Brussels, Belgium

[3]Сочинский научно-исследовательский центр РАН

Статья поступила в редакцию 15 июня 2007 г.
Представлена членом редколлегии А.Ф. Глазовским

Рассмотрена чувствительность модельной хронологии льда в нижней части керна EDML, полученного на станции Конен в Антарктиде, к вариациям потока геотермического тепла.

Introduction

Deep drilling of the Antarctic ice sheet at Kohnen station (Dronning Maud Land, DML) finished in January 2006. It was conducted within the framework of the European Project for Ice Coring in Antarctica (EPICA) and aimed at obtaining high-resolution proxy records for the last glacial cycle. Accurate dating of an ice core is an important condition for the correct interpretation of physical and chemical properties of ice core records in terms of climate change. Dating of the EDML ice core was carried out by means of synchronization with established ice-core chronologies [3, 4]. Independent ice-core dating was performed in [1] by means of glaciological modelling using a 3-D nested Antarctic ice sheet model. Both methods provided a similar depth-age scale for the upper ~9/10 of the EDML ice core. Dating of the lower part of the core requires future efforts in understanding how the age of the ice in the lower part of the EDML ice core depends on the major unknown variable, the geothermal heat flux (G).

The geothermal heat flux influences the lower boundary of an ice sheet by controlling the temperature conditions at the ice sheet/ bedrock interface [6, 9]. Though variations of G do not drastically affect global characteristics of ice sheets such as total ice volume and ice sheet extent (see a review by Pollard et al. [16]) they determine the extent of the basal area over which melting takes place [8]. Tarasov and Peltier [21] established that for values of G around 50 mWm^{-2} (a value close to the characteristic value for Antarctica, see below), a 1 mWm^{-2} increase in G leads to a 0.4°C increase in present-day modeled basal temperature. Though their result was obtained for the Greenland ice sheet summit, it clearly pointed out how crucial it is to determine G in ice-sheet studies as accurately as possible.

There are very few direct measurements of G. Most of them come from rock outcrops near the edge of the continent or from the ocean margins [12], or they have been inferred from the few deep drilling sites which reached bedrock [18]. Therefore in ice-sheet modeling one has to rely on indirect estimates based on a variety of approaches. Approaches based on tectonic regionalization consist of outlining typical geological structures, and extrapolating the characteristic G of these structures to the region of interest. For instance, according to Pollack et al. [15] G and its standard deviation for a typical East Antarctic Proterozoic unit is 58.3±23.6 mWm^{-2}, and in Archean units it is 51.5±25.6 mWm^{-2}. Llubes et al. [12] used the typical values of G derived by Pollack et al. [15] and the geological map of Antarctica by Borg et al. [2] to reconstruct a schematic map of G for all of Antarctica. In their representation G increases from 51 mWm^{-2} in the coastal zone of East Antarctica to 69 mWm^{-2} at the northern margin of West Antarctica. On their map, the area around Kohnen station in DML lies on the boundary between Proterozoic and Archean units. This boundary position of Kohnen increases the uncertainty of estimates for G in that area.

Shapiro and Ritzwoller [20] considered that the approach based on geological structuring is not ideal for Antarctica because Antarctic tectonics is not well understood. They suggested an approach based on seismic modeling. This approach provides the general features of G but does not give variations below spatial scales of several tens of kilometres (see Fig. 8a in the referenced paper). Moreover, standard deviations of G obtained using this approach are in fact comparable to G itself. In DML G varies within the limits ~50-65 mWm^{-2}, a somewhat higher estimate compared to the one predicted by Pollack et al. [15]. The estimate of the standard deviation of G in DML by Shapiro and Ritzwoller [20] of 20-35 mWm^{-2} is also somewhat higher compared to estimates by Pollack et al. [15].

Shapiro and Ritzwoller [20] furthermore pointed out that it is necessary to take into account the crustal contribution to heat flow through the decay of radioactive elements. This input can be rather variable in space at scales of tens of kilometres. This scale is not resolved within the seismic approach.

Using the example of Scandinavia, Näslund et al. [13] demonstrated that the field of G can be of a mosaic character with a rather high variability from one point to another. Such a patchy structure of the G-field under Antarctica was experimentally established by Fox Maule et al. [5]. They implemented a method to estimate G using satellite magnetic data. According to their reconstructions, G varies in the surroundings of Kohnen within the limits of approximately 55-70 mWm^{-2}. The error on their model estimates of G is rather high (21-27 mWm^{-2}), but is comparable to the standard deviations of G obtained by Pollack et al. [15] and by Shapiro and Ritzwoller [20].

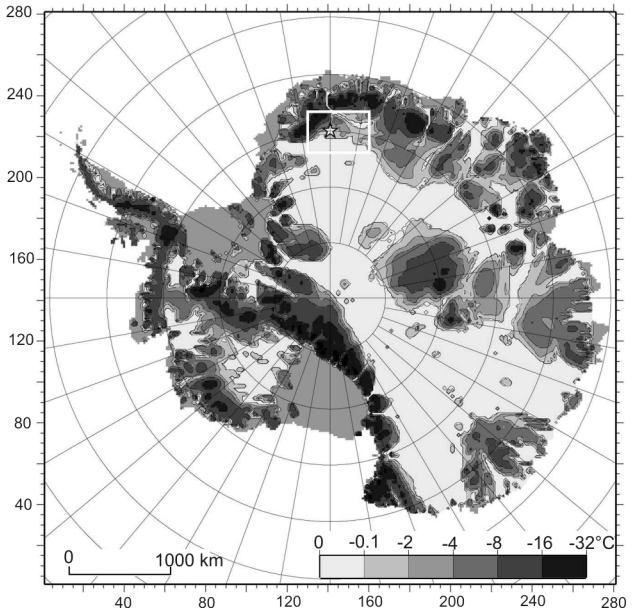

Fig. 1. Model derived basal temperature, °C, relative to pressure melting. Outlined as a white rectangle is the region of interest around Kohnen station (shown as a star)

Рис. 1. Рассчитанная в модели современная базальная температура с учетом поправки на давление(°C) .Белым прямоугольником показан район исследований, белой звездочкой – станция Конен

None of the methods mentioned above gives a G estimate in DML with an accuracy better than ~30%. According to numerical experiments with G=54.6 mWm^{-2}, considered a mean value for all of Antarctica [19], basal melting at Kohnen occurred for most of the time during the past several glacial cycles but ceased nearly 7 kyr ago. Nevertheless, during drilling of the deeper layers at Kohnen melt water was found. This suggests that melting still takes place at the present day at the drill site. Alternatively, it could also mean that the temperature has remained so close to the pressure melting point during the last few thousand years that the phase transition barrier could not be overcome. In both cases, however, the value of G is probably somewhat higher than the one adopted in the reference model. To clarify the influence of G on the depth-age distribution in the lower segment of the EDML ice core we carried out a series of numerical experiments with G higher than the reference value of 54.6 mWm^{-2} (G_{ref}) by an amount between 2 and 30%.

Modeling methodology

The formulation of the 3-D ice sheet model is basically identical to that described in [10, 11]. Ice is considered as an incompressible viscous non-Newtonian fluid. Ice-flow dynamics is described within the framework of the Shallow Ice Approximation, SIA [7]. The model generates the ice-sheet geometry, solid earth response, the surface temperature and the surface mass balance. Thermomechanical coupling is described by a temperature dependent rate factor in Glen's flow law with exponent n=3. The model equations are solved with the finite difference method on a regular grid of 281×281 points with a horizontal resolution of 20 km. There are 30 layers in the vertical, which are unequally spaced with smaller steps near the bottom of the ice sheet. The vertical coordinate is dimensionless – it is scaled by the local ice thickness. Ice temperature, T_{ice}, is determined by the expression:

$$\frac{\partial T_{ice}}{\partial t} = \frac{1}{\rho_{ice} c_p} \frac{\partial}{\partial z}\left(k_{ice} \frac{\partial T_{ice}}{\partial z} \right) - \mathbf{v}\nabla T_{ice} + \frac{2\dot{\varepsilon}\tau}{\rho_{ice} c_p}, \qquad (1)$$

where ρ_{ice} is the density of ice, c_p is specific heat capacity, k_{ice} is thermal diffusivity, $\mathbf{v}$ is the 3-dimensional velocity field, $\dot{\varepsilon}$ is effective strain rate, τ is effective deviatoric stress. The first term on the right hand side describes diffusion, the second one – advection, and the third one – dissipation of heat. The geothermal heat flux enters (1) through formulation of the boundary condition at the bedrock/ice sheet interface, i.e. from the condition of continuity of temperature gradients across this boundary: $\frac{\partial T_{ice}}{\partial z} = \frac{\partial T_{rock}}{\partial z} = \frac{k_{rock}}{k_{ice}} \frac{\partial T_{rock}}{\partial z} + \frac{\tau_{base}\mathbf{v}}{k_{ice}}$, where T_{rock} is the temperature of the underlying bedrock and k_{rock} is the thermal conductivity of bedrock. On the lower bedrock boundary $\frac{\partial T_{rock}}{\partial z} = \frac{G}{k_{rock}}$ (see details in [8, 9]. As mentioned above, G= 54.6 mWm^{-2} in the reference run.

The duration of all numerical experiments was 740 kyr. The age of the ice (time of deposition at the surface of the ice sheet) was calculated using Lagrangian back-tracing of an ice particle in the time-dependent 3D velocity field. This procedure is described in [1]. Virtual ice particles (tracers) are placed in the vertical at the exact geographical position of the drill site every 0.1% of relative ice-equivalent depth between 0.1% and 99.9%. The components of the horizontal velocity u and v, basal melting at the bed S, surface topography s and ice thickness h are first computed in a forward experiment and stored every 100 model years (Δt) for the area corresponding to the sub-domain (Fig. 1), which is big enough to embed all possible trajectories of the tracers. The velocity at the particle's position is calculated using 3D-splines, other fields – by 2D-splines [17]. The time t when an ice particle crosses the surface of the ice sheet is fixed and accepted as the time of deposition. Similarly, x and y-coordinates of the place where a tracer crosses the surface is accepted as the place of deposition.

The vertical velocity field $w(x,y,h)$ is calculated from the continuity equation with boundary conditions taken either at the surface h or at the bottom b:

$$w(h) = \frac{\partial h}{\partial t} + u(h)\frac{\partial h}{\partial x} + v(h)\frac{\partial h}{\partial y} - M_h - M_b,$$

where $h(x,y)$ is the surface topography and M_h is the surface mass balance. Since no ablation occurs in Antarctica, M_h equals the accumulation rate. At the bottom (bedrock/ice sheet interface), the alternative kinematic boundary condition is:

$$w(b) = \frac{\partial b}{\partial t} + u(b)\frac{\partial b}{\partial x} + v(b)\frac{\partial b}{\partial y} - M_b,$$

where $b(x,y)$ is the bedrock topography and M_b is the mass balance at the bottom of the ice sheet. The latter is equal to the basal melting rate, $M_h \equiv S$:

$$S=\frac{1}{\rho_w L}\left[k_{ice}\left(\frac{\partial T_{ice}}{\partial z}\right)_{base}-k_{rock}\left(\frac{\partial T_{rock}}{\partial z}\right)_{upper}-\tau_{base}\mathbf{v}\right]+\frac{2}{\rho_w L}\int_h^{z_{melt}}\dot{\varepsilon}\tau dz,$$

where ρ_w is the density of water, L is the latent heat of melting, τ_{base} is the shear stress vector at the bottom, and z_{melt} is the upper boundary of a temperate basal layer, which may eventually develop in the calculations and assumes that all produced melt water is drained away at the base.

Sensitivity of the basal temperature, basal melting rate, and basal ice age to *G*

Fig. 1 shows the modelled present-day Antarctic basal temperature relative to pressure melting point (*pmp*) calculated assuming steady state conditions. The region of particular interest is located in Dronning Maud Land and has dimensions 600×400 km (outlined in white in Fig.1). Apparently, the temperature field is rather complex, and Kohnen station lies close to the boundary of a large area at pressure melting. To understand how basal conditions depend on G we carried out a series of time-dependent numerical experiments in which G was increased stepwise by 2 to 30%. In the reference experiment the ice is frozen to the bed ($T_{pmp}=-0.2$°C). The same is still true when G is increased by only 2%. With G increased by 5% above the reference value, present-day Kohnen ice is already at pressure melting (Table1).

Alongside with increases in G, the ice thickness at Kohnen decreases. To keep ice thickness as close as possible to the observed one to eliminate unwanted feedbacks on basal temperature, we reduced the softness of the ice. Glen's flow law links stresses to strain rates, $\tau_{ij}=2\eta\dot{\varepsilon}_{ij}$, where

$$\eta=\frac{1}{2}A(\theta^*)^{-1/n}\dot{\varepsilon}_e^{(1-n)/n},$$

$\dot{\varepsilon}_e$ is the effective strain rate, and $A(T^*)$ is the rate factor, which is a function of temperature corrected for the pressure melting point:

$$A(T^*)=Ea\exp\left(-\frac{Q}{RT^*}\right). \qquad (2)$$

In Equation (2) Q is the thermal activation energy of creep, R is the universal gas constant, a – is a constant, and E is the enhancement factor. The enhancement factor is a non-dimensional multiplier describing the increase or decrease in strain rate caused by (unknown) variations in crystal size, impurity content and crystal orientation [14]. In this study we tune E in a way that the model produces thicknesses close to the real ice thickness in the grid point closest to the EDML coordinates (this node is located nearly 2.55 km north-west from the position of Kohnen).

Table 1

Modeled present-day characteristics at EDML using a constant enhancement factor $E=0.78$*

Experiment	G	S, m	H, m	T_{pmp}, °C	S_m, mm yr^{-1}	ΣS_m, m
Exp1	Reference	2884	2745	-0.20	0.00	40
Exp2	+2%	2879	2736	-0.10	0.00	162
Exp3	+5%	2831	2678	*pmp*	0.07	289
Exp4	+10%	2814	2651	*pmp*	0.46	460
Exp5	+15%	2787	2613	*pmp*	0.70	645
Exp6	+20%	2771	2590	*pmp*	0.98	829
Exp7	+25%	2751	2563	*pmp*	1.22	1011
Exp8	+30%	2729	2533	*pmp*	1.47	1196

*G – geothermal heat flux, S – surface elevation in metres above sea level, H – ice thickness, T_{pmp} – basal temperature relative to pressure melting, S_m – basal melting rate, ΣS_m – total cumulated loss of ice at the base over 740 kyr.

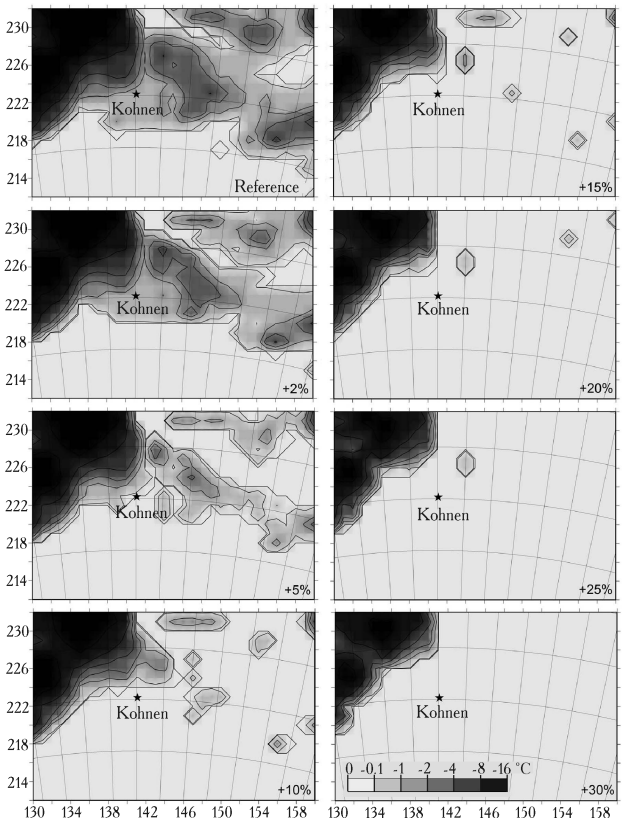

Fig. 2. Modelled present-day temperatures of basal ice relative to pressure melting point (°C) in numerical experiments *i* with $G_i=G_{ref}=5...30\%$, where $G_{ref}=56.4$ mWm^{-2} is the value of the geothermal heat flux in the reference experiment. The decrease in ice thickness due to basal melting is compensated by tuning the enhancement factor (E) in the flow law.

Рис. 2. Рассчитанная в модели современная базальная температура с учетом поправки на давление (°C) в численных экспериментах i, при $G_i=G_{ref}=5...30\%$, где $G_{ref}=56.4$ mWm^{-2} – стандартное значение потока геотермического тепла. Снижение толщины льда вследствие базального таяния компенсируется уменьшением множителя E в законе растекания

Ice-equivalent thickness at Kohnen can be estimated as 2745.38 m. It is equal to 2774 m (real depth of the borehole close to the bottom where drilling was stopped due to appearance of meltwater, *F. Wilhelms, personal communication*) minus 28.62 m of ice equivalent depth resulting from compaction of the overlying firn layer. This is considered to be the lowest possible limit, because drilling did not reach the bedrock. This value was adopted as a conventional ice thickness and a target value. The purpose was to tune E so that H_i would not differ from H_{obs} by more than 1%, i.e. should lie within the limits ~2718-2773. In the reference model run $E=0.78$ yields a realistic ice thickness.

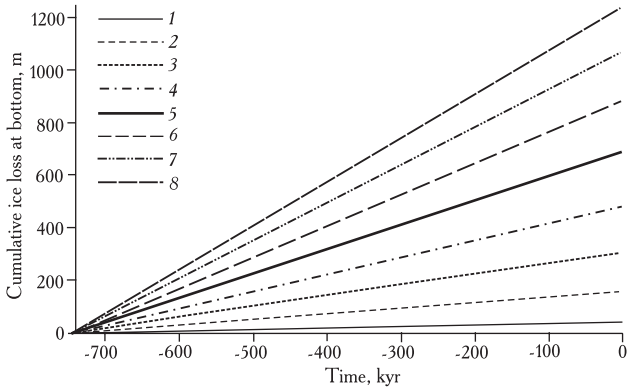

Fig. 3. Cumulative ice loss ($\sum S_i$, m) at the base of the ice sheet at Kohnen over 740 kyr of integration in the numerical experiments

Рис. 3. Суммарная потеря льда ($\sum S_i$, м) на нижней границе ледникового щита на станции Конен в течение 740 тыс. лет в численных экспериментах. Геотермический поток тепла: *1* – стандартное значение, *2* – +2%, *3* – +5%, *4* – +10%, *5* – +15%, *6* – +20%, *7* – +25%, *8* – +30%

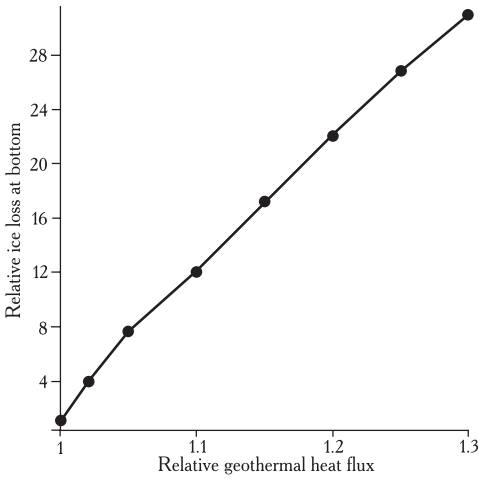

Fig. 4. Dependence of the relative ice loss $\sum S_i / S_{ref}$ on the relative geothermal heat flux G_i / G_{ref} ($\sum S_i$ is the loss in experiment *i* with geothermal heat flux G_i, $\sum S_{ref}$ is the loss in the reference experiment with a reference value G_{ref})

Рис. 4. Зависимость относительной потери льда $\sum S_i / S_{ref}$ от относительного потока геотермического тепла G_i / G_{ref} ($\sum S_i$ – потеря льда в эксперименте i при значении потока геотермического тепла G_i, $\sum S_{ref}$ – в стандартном эксперименте при значениим потока геотермического тепла G_{ref})

The relation between E and present-day H is not straightforward, because changes of E influence the dynamical history of the ice sheet due to feedbacks between ice thickness, isostasy, accumulation rate, 3-D velocity field, and ice temperature. Direct inference of the exact value of E that fits the desired value of H is hardly possible. Table 2 shows a number of model-derived characteristics obtained with a specific E selected to best approach H.

Shown in Fig. 2 are also the fields of the temperature relative to the pressure melting point (T_{pmp}). Increasing G by 2% does not result in present-day basal melting at Kohnen. With increasing G the frozen area decreases rather fast, and with G_{ref}+5% the melting area already encompasses Kohnen. When G reaches the maximum examined value (G_{ref}+30%) the melting area expands over the whole region with the exception of the northwestern corner, where the ice is much thinner.

Integration of the basal melting rate through time yields the total loss of bottom ice from the EDML drill site (Fig. 3). In the reference experiment, where the pressure melting point is hit intermittently, this loss is lower than 50 m during 740 kyr. The total loss increases almost linearly with increasing G, with somewhat higher rates during the transition from G_{ref} to G_{ref}+2% (Fig. 4). In the case of G_{ref}+30% the total loss over the calculation period increases to ~1200 m (see Table 2). Tuning of E results in an increase of total ice loss by 4-6% compared to experiments with untuned E (see the last columns in Tables 1 and 2).

Table 2

Modeled present-day characteristics at EDML using E tuned to fit the observed ice equivalent H at Kohnen*

Experiment	G	E	S, m	H, m	T_{pmp}, °C	S_m, mm yr^{-1}	ΣS_m, m
Exp1	Reference	0.78	2884	2745	-0.20	0.00	40
Exp2	+2%	0.70	2876	2736	-0.21	0.00	159
Exp3	+5%	0.59	2863	2724	*pmp*	0.07	307
Exp4	+10%	0.41	2892	2757	*pmp*	0.68	481
Exp5	+15%	0.22	2879	2747	*pmp*	0.77	689
Exp6	+20%	0.15	2875	2745	*pmp*	1.06	882
Exp7	+25%	0.09	2868	2739	*pmp*	1.30	1071
Exp8	+30%	0.08	2880	2750	*pmp*	1.63	1241

*Notations used are the same as in Table 1.

The age of the ice in the lower parts of the core is inevitably affected by basal melting. Fig. 5a shows the depth-age profiles calculated under different assumptions for the value of G. Apparently, all curves are very close to each other beginning from the top down to ~89% of relative depth. Below this point the depth-age curves start to diverge. This is illustrated in detail in Fig. 5b, where depth-age distributions are shown for the lowermost 5% of the core. With G_{ref}+2% the ice is still frozen to the bottom, and the form of the age curve is similar to the reference curve. With G_{ref}+5%, when the basal ice is melting also at present day, the ice age reduces from nearly 736 kyr to nearly 390 kyr at 99.8% relative depth. With further increases of G to G_{ref}+30% the age at 99.8% relative depth becomes another 150 kyr 'younger'. The change of the rate of age decrease is illustrated in Fig. 6, which shows a rather abrupt decrease of the bottom ice age with increasing G to G_{ref}+5%, and a more gradual decrease during the transition from G_{ref}+5% to G_{ref}+30%. This abrupt increase is explained by the geographical expansion of the melting area to Kohnen, which happens when G increases to G_{ref}+5%.

Concluding remarks

In this study we examined the effect of uncertainties in G on the model-derived basal temperature conditions and the ice chronology in the lowermost part of the EDML ice core. The value of G beneath the Antarctic ice sheet is large-

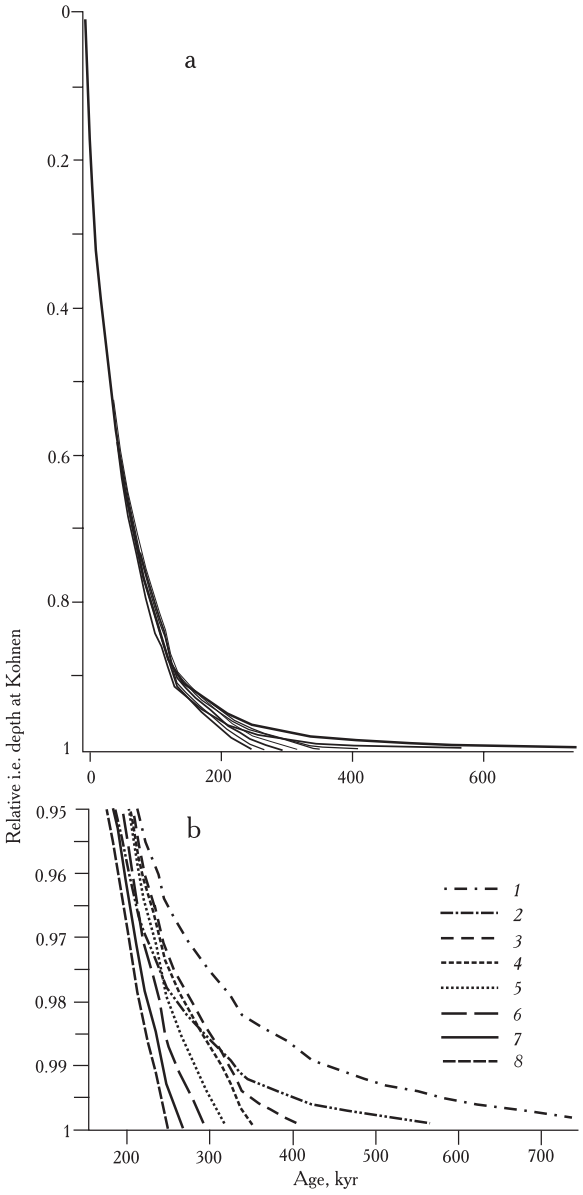

Fig. 5. Depth-age distribution in the EDML ice core derived by Lagrangian back-tracing in the numerical experiments under different assumptions of G. Down to ~90% of relative ice equivalent depth all curves are very close to each other but they start to diverge further below

Рис. 5. Кривые распределения возраста в керне EDML, полученные с использованием лагранжева метода обратного отслеживания в численных экспериментах с различными значениями G. До горизонта ~90% (а) относительной глубины в ледовом эквиваленте все кривые лежат очень близко друг к другу, а ниже начинают расходиться (б): геотермический поток тепла: *1* – стандартное значение, *2* – +2%, *3* – +5%, *4* – +10%, *5* – +15%, *6* – +20%, *7* – +25%, *8* – +30%

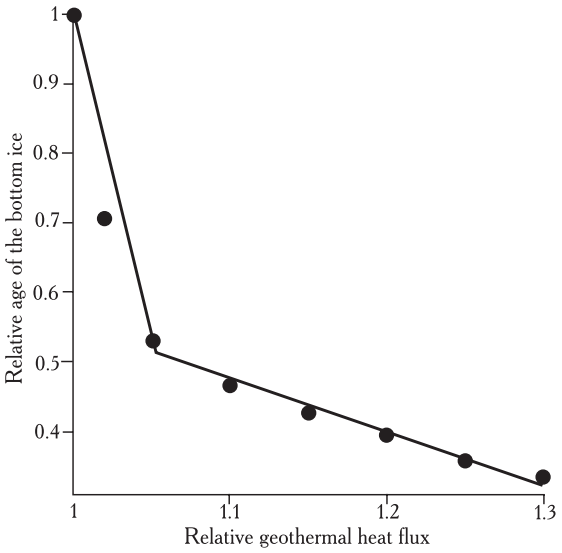

Fig. 6. Dependence of the relative age at 99.8% of relative ice equivalent depth (A_i/A_{ref}, where A_{ref} is age of the ice in the reference experiment) on the relative geothermal heat flux (G_i/G_{ref}).

Рис. 6. Зависимость относительного возраста льда (99,8% относительной глубины в ледовом эквиваленте) A_i/A_{ref}, где A_{ref} – возраст в стандартном эксперименте, от относительного потока геотермического тепла (G_i/G_{ref}, обозначения см. на рис. 2)

ly unknown and can only be estimated indirectly. None of the indirect methods provides an accuracy better than approximately one-third of the characteristic value of *G*. An additional complication is the location of Kohnen station in a region where two geologic units meet. These units, Proterozoic and Archean, have a different characteristic *G*. In addition, local variations of *G* in Dronning Maud Land are possibly high at a spatial scale of tens of kilometres.

The exact knowledge of *G* is not crucial for glaciological dating of the upper ~89% of the EDML ice core. Below this depth *G* becomes the most important factor determining basal temperature, basal melting rate, and hence vertical velocity of the ice. Increasing *G* by only 5% with respect to the reference value of 54.6 mWm^{-2} for Antarctica results in present-day basal melting. The threshold between melting and non-melting conditions at the ice sheet/ bedrock interface below Kohnen lies within the limits of 57.6 and 59.2 mWm^{-2}.

For the range of values of *G* tested in this paper, the ice age at 99.8% relative depth varies between 736 kyr and 240 kyr. It is our strategy to compare these modeling scenarios with fixed points (terminations) derived from synchronization with other ice core or marine records to assess the likelihood of specific dating possibilities. In the current research we outlined only the contours of these future activities. The latter will consist in the application of a higher-order and higher-resolution nested model to produce the most accurate version of the ice core chronology for the lower part of the EDML ice core.

Acknowledgements

The authors wish to thank Klaus Ketelsen (DKRZ) for essential help to adjust the model code for highly productive parallel computations, Frank Wilhelms (AWI) for providing the EDML borehole temperatures to compare with our model results, and Chris Zweck (University of Arizona) for making valuable remarks to improve the manuscript. The Belgian Programme on Science for a Sustainable Development (Belgian Federal Science Policy Office)

supported part of the work under contract SD/CA/02A (ASPI). This work is a contribution to the European Project for Ice Coring in Antarctica (EPICA), a joint European Science Foundation/European Commission scientific programme, funded by the EU and by the national contributions from Belgium, Denmark, France, Germany, Italy, the Netherlands, Norway, Sweden, Switzerland and the United Kingdom. The main logistic support was provided by IPEV and PNRA (at Dome C) and AWI (at Dronning Maud Land). This is EPICA publication no. XXX.

REFERENCES

1. *Рыбак О., Хёбрехтс Ф., Пагген Ф., Штайнхаге Д.* Региональня модель динамики льда. Часть 2. Постэкспериментальная обработка данных. — МГИ, вып. 103, 2007, с. 3-10.
2. *Borg S.G., De Paolo D.J., Smith B.M.* Isotopic structure and tectonics of the central Transantarctic Mountains. — Journ. of Geophys. Research, v. 95(B5), 1990, p. 6647-6667.
3. EPICA community members. Eight glacial cycles from an Antarctic ice core. — Nature, v. 429, 2004, p. 623-628.
4. EPICA community members. One-to-one interhemispheric coupling of polar climate variability during the last glacial. — Nature, v. 444, 2006, p. 195-198.
5. *Fox Maule C., Purucker M.E., Olsen N., Mosegaard K.* Heat Flux Anomalies in Antarctica Revealed by Satellite Magnetic Data. — Science, v. 309, 2005, p. 464-467.
6. *Greve R.* Relation of measured basal temperatures and the basal distribution of the geothermal heat flux for the Greenland ice sheet. — Annals of Glaciology, v. 42, 1995, p. 424-432.
7. *Hutter K.* Theoretical Glaciology: material science of ice and the mechanics of glaciers and ice sheets. D. Reidel Publishing Co, Dordrecht etc, 1983, 510 p.
8. *Huybrechts P.* The Antarctic ice sheet and environmental change: a three-dimensional modelling study. Berichte zur Polarforschung, v. 99, 1992, 241 p.
9. *Huybrechts P.* Basal temperature conditions of the Greenland ice sheet during the glacial cycles. — Annals of Glaciology, v. 23, 1996, p. 226-236.
10. *Huybrechts P.* Sea-level changes at the LGM from ice-dynamic reconstructions of the Greenland and Antarctic ice sheets during the glacial cycles. — Quaternary Science Reviews, v. 21, 2002, p. 203-231.
11. *Huybrechts P., de Wolde J.* The Dynamic Response of the Greenland and Antarctic Ice Sheets to Multiple-Century Climatic Warming. — Journ. of Climate, v. 12, 1999, p. 2169-2188.
12. *Llubes M., Lanseau C., Rémy F.* Relations between basal condition, subglacial hydrological networks and geothermal heat flux in Antarctica. — Earth and Planetary Science Letters, v. 241, 2006, p. 655-662.
13. *Näslund J.-O., Jansson P., Fastook J.L. et al.* Detailed spatially distributed geothermal heat-flow data for modeling of basal temperatures and meltwater production beneath the Fennoscandian ice sheet. — Annals of Glaciology, v. 40, 2005, p. 95-101.
14. *Pettit E.C., Waddington E.D.* Ice flow at low deviatoric stress. — Journ. of Glaciology, v. 49, 2003, p. 359-369.
15. *Pollack H.N., Hurter S.J., Johnson J.R.* Heat flow from the Earth's interior: analysis of the global data set. — Reviews of Geophysics and Space Physics, v. 31(3), 1993, p. 267-280.
16. *Pollard D., DeConto R.M., Nyblade A.A.* Sensitivity of Cenozoic Antarctic ice sheet variations to geothermal heat flux. — Global and Planetary Change, v. 49, 2005, p. 63-74.
17. *Press W.H., Teukolsky S.A., Vetterling W.T., Flannery B.P.* Numerical Recipes, 2nd ed. Cambridge, Cambridge University Press, 1992, 963 p.
18. *Ritz C.* Interpretation of the temperature profile measured at Vostok, East Antarctica. — Annals of Glaciology, v. 12, 1989, p. 138-144.
19. *Sclater J.G., Jaupard C., Galson D.* The heat flow through oceanic and continental crust and the heat loss of the Earth. — Reviews of Geophysics and Space Physics, v. 18(1), 1980, p. 269-311.
20. *Shapiro N.M., Ritzwoller M.* Inferring surface heat flux distributions guided by a global seismic model: particular application to Antarctica. — Earth and Planetary Science Letters, v. 223, 2004, p. 213-224.
21. *Tarasov L., Peltier W.R.* Greenland glacial history, borehole constrains, and Eemian extent. — Journ. of Geophys. Research, v. 108(B3), 2003, doi:10.1029/2001JB001731.

ЧУВСТВИТЕЛЬНОСТЬ ХРОНОЛОГИИ КЕРНА EDML К ГЕОТЕРМИЧЕСКОМУ ПОТОКУ

В 2001-2006 гг. в рамках проекта EPICA (European Project for Ice Coring in Antarctica) на станции Конен (75°00′.104 ю.ш., 0°04′.07 в.д) на Земле Королевы Мод в Антарктиде было выполнено глубокое бурение. Ключевая проблема интерпретации данных любого ледяного керна состоит в построении реалистичной хронологии. К настоящему времени выполнено датирование около 9/10 керна EDML с использованием метода синхронизации с другими кернами и гляциологического метода. Ниже указанного горизонта результаты датирования с помощью метода гляциологического моделирования в значительной степени зависят от принятого значения потока геотермического тепла (G). Обнаруженная в ходе бурения в слоях льда вблизи подстилающих пород талая вода свидетельствует о придонном таянии, т.е. принятое в численных экспериментах стандартное значение $G = 54{,}6$ mWm^{-2} для окрестностей станции Конен занижено. Существующие методы косвенной оценки величины G под ледниковым щитом Антарктиды не позволяют определить ее с ошибкой менее 30%. В то же время даже небольшое увеличение значения G приводит к значительным изменениям базальных условий. Чтобы выяснить чувствительность придонного распределения возраста льда в керне к вариациям потока геотермического тепла, мы выполнили серию численных экспериментов, в которых значение G было выше стандартного на 2-30%.